Thermotidal and land-heating forcing of the diurnal cycle of oceanic surface winds in the eastern tropical Pacific

Ken Takahashi[1]

Submitted: December 18, 2011; Revised: January 19, 2012; Accepted: January 24, 2012

The diurnal cycle in the oceanic surface winds in the tropical eastern Pacific is shown, through numerical experiments with a regional atmospheric model, to be associated with the migrating diurnal atmospheric thermal tide, forced by absorption of solar near-IR radiation by tropospheric water vapor, and a topographically-modified extended sea-breeze, forced by diurnal land heating.

Idealized experiments prove capable of discriminating the effects of both processes, showing that beyond 2000 km from the coast, the thermal tide is dominant, while closer to the coast both processes are of the same order.

The shortwave forcing due to water vapor is also found to produce a diurnal cycle in precipitation, but the process appears to be independent from the thermal tide and it is proposed that this effect is mediated by the radiatively-forced changes in the column stability.

1. Introduction

The diurnal cycle of surface winds near coasts can be described as the response to the diurnal solar heating of the coastal land surfaces, leading to an extended sea breeze circulation [e.g. *Gille et al.*, 2003]. In the southeast Pacific, the diurnal cycle in vertical velocity, which affects the boundary layer structure and cloud properties, is associated with a southwestward propagating wave ultimately forced by the diurnal heating of the Andes [*Garreaud and Muñoz*, 2004; *Wood et al.*, 2009; *Rahn and Garreaud*, 2010].

On the other hand, although the extended sea-breeze can be expected to propagate off-shore through wave dynamics [*Rotunno*, 1983], the observed diurnal cycle in the near-equatorial oceans is rather zonally uniform [*Deser and Smith*, 1998; *Dai and Deser*, 1999; *Gille et al.*, 2003; *Ueyama and Deser*, 2008] and its offshore extent cannot be explained by simple sea breeze models [e.g. *Yan and Anthes*, 1987].

In the tropical Pacific, the structure of the diurnal cycle in surface winds presents approximate a mirror symmetry with respect to the equator, with maximum poleward anomalies around 07 LT (local time) accelerated to a large extent by meridional pressure gradients, which in turn could be associated with the radiatively-driven diurnal migrating (i.e. propagating westward with the subsolar point) atmospheric tide [*Ueyama and Deser*, 2008], mainly due to shortwave absorption by tropospheric water vapor [e.g. *Lindzen*, 1967].

In the present study we perform experiments with a full-physics regional numerical atmospheric model to assess the forcing mechanisms of the diurnal cycle in near-surface winds in the eastern tropical Pacific. In particular, the relative roles of the atmospheric thermal tides and diurnal land heating are assessed with controlled experiments in which each forcing is suppressed.

2. Model and experiments

This study uses the Fifth Generation PSU/NCAR Mesoscale Model (MM5) v.3.7 non-hydrostatic regional atmospheric model [*Grell et al.*, 1995]. The domain was configured with 28 time-invariant terrain-following σ levels, with the highest level at a reference pressure of 50 hPa, including the eastern Pacific, Central America, and western South America (50°S-35°N, 168°W-52°). Although the grid size of $\Delta x \approx 120$ km is adequate for the diurnal gravity wave off southern Peru/northern Chile (wavelength ~ 2000 km, *Garreaud and Muñoz* [2004]; *Rahn and Garreaud* [2010]) and for the migrating diurnal tide (wavelength = circumference of Earth), it does not resolve coastally-trapped sea-breeze circulations (scale $\sim 100-200$ km, e.g. *Arritt* [1989]; *Simpson* [1994]), which are expected to occur polewards of 30°.

Among the parametrization schemes, of particular relevance to the experiments is the use of the CCM2 radiation code [*Hack et al.*, 1993], with explicit shortwave absorption by different species, and the force-restore soil slab model for ground temperature [*Blackadar*, 1976], in which the slab heat capacity and the rate of relaxation to a reservoir temperature are tuned to mimic the diurnal cycle of a multilayer soil model. The schemes used for boundary layer and cumulus convection are Gayno-Seaman [*Gayno*, 1994] and Grell [*Grell*, 1993], respectively.

The control experiment (CTL) was performed for October 2008, but the initial and lateral boundary conditions were set to the monthly-averaged NCEP/NCAR Reanalysis data for that month and sea surface temperature was fixed to the NOAA OI SST estimate for the first week of October 2008. This procedure excludes external sources of variability (diurnal and synoptic), allowing for a larger signal-to-noise ratio and cleaner attribution to the forcings, while weakly affecting the monthly mean and composite diurnal cycle of the simulations (the results are qualitatively similar to an otherwise equal run using the 6-hourly data for 1-31 October 2008). Lateral boundary conditions are implemented through relaxation to the boundary values within a 4-grid point layer. Output was obtained every two hours and the first two days of the simulations were discarded to allow for the spin-up of the atmosphere. The composite daily cycle and the corresponding diurnal harmonic coefficients were calculated from the remainder of the simulations.

The perturbed runs are the same as CTL with the following exceptions. In the HIC experiment the diurnal cycle in land surface temperature is reduced by increasing by a factor of 100 the soil heat capacity (C) in the slab soil model $CdT/dt = Q - \lambda(T - T_s)$, where T and T_s are the surface and (prescribed) reservoir temperatures, respectively, Q is the net surface heat flux, and λ is a constant coefficient (the adjustment time scale of the slab temperature increases to

[1]Instituto Geofísico del Perú, Lima, Perú

0094-8276/12/$5.00

$\sim$ 2 days in this case). In the NOH2OABS experiment the atmospheric absorption of shortwave radiation by water vapor is suppressed by setting the corresponding absorption coefficients to zero in the CCM2 radiation code. Sensitivity to the cumulus parameterization scheme was tested by making runs similar to the above but using with the *Kain and Fritsch* [1993] scheme instead of Grell.

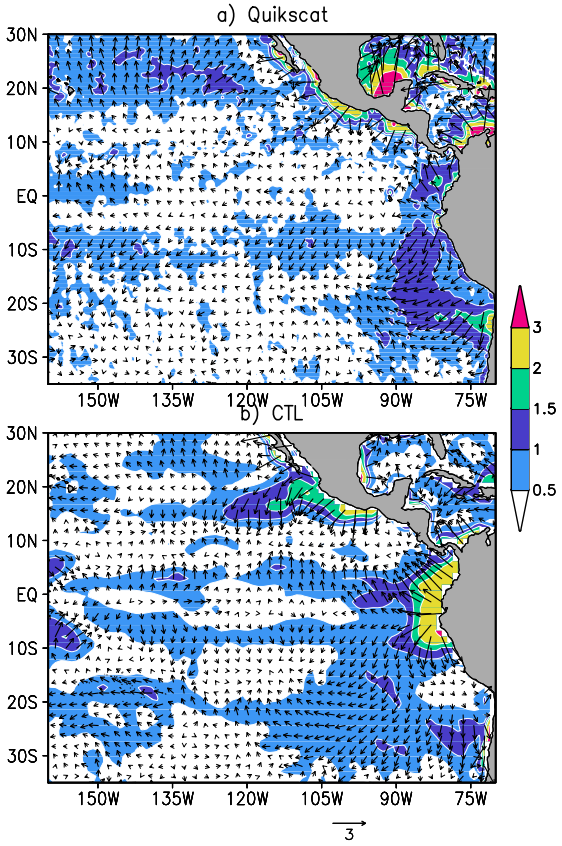

Figure 1. a) Observed mean morning ($\sim$6 LT) minus evening ($\sim$18 LT) scatterometer surface wind vector difference and its magnitude (m/s) from Quikscat ascending and descending passes (September-November 2008). b) Similarly, for the wind at the $\sigma = 0.995$ level (32 masl) from the CTL run reconstructed from the diurnal harmonics. Vectors are shown every few grid points.

3. Analysis and results

In Fig. 1a we show the mean morning minus afternoon difference in surface wind from Quikscat scatterometer in the eastern Pacific (cf. *Gille et al.* [2003]). In general, the vectors point away from the coastlines (Fig. 1a), as would be expected from gravity waves driven by land cooling/heating and propagating away from the continent, except near the coast between 20 and 30°S, where the vectors are southward. The highest magnitudes are located within 1000 km from the coast except for the offshore maximum between 10 and 20°S, which *Gille et al.* [2003] speculate is associated with the blocking effect of the Andes. South of Panama ($\sim$ 7°N), the maximum magnitudes are typically between 1 and 2 m/s, but north of this they are higher than 2 m/s within 200 km from the coasts. Zonal bands with poleward vectors are found on both sides of the equator in scatterometer data [*Gille et al.*, 2003, Fig. 1a] and the TAO buoy array [*Deser and Smith*, 1998; *Ueyama and Deser*, 2008].

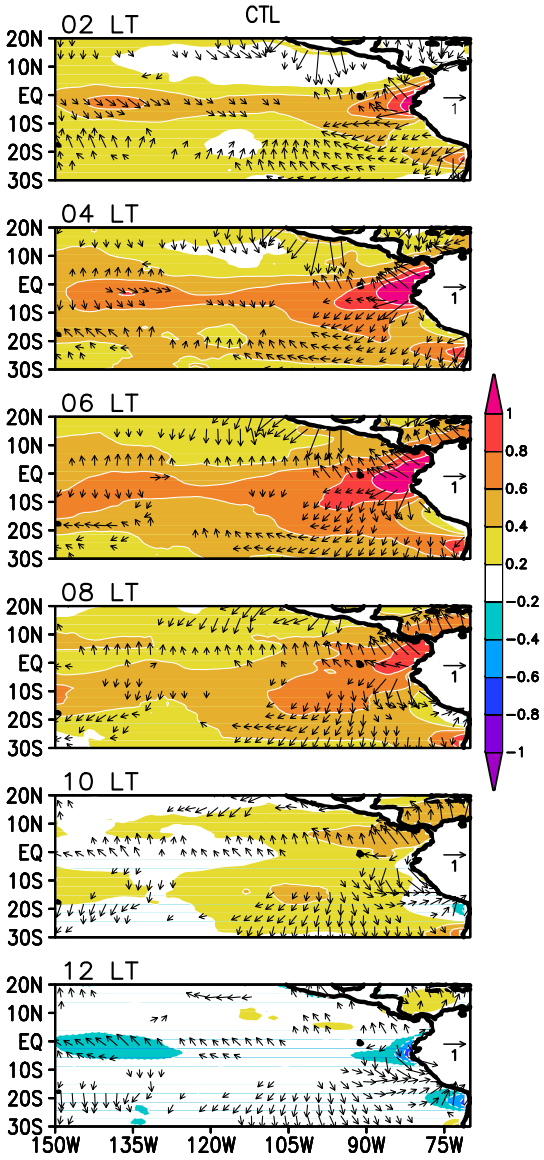

Figure 2. Anomalies from the daily mean in oceanic $\sigma = 0.995$ wind (m/s) and pressure (hPa) at 02, 04, 06, 08, 10 and 12 local time, reconstructed from the diurnal harmonics of the CTL simulation.

The CTL simulation reproduces most of these features (Fig. 1b). The zonal band along 10°S with southward vectors extends across the Pacific and has a counterpart with northward vectors in the northern hemisphere (cf. Fig. 2 in *Gille et al.* [2003], and *Ueyama and Deser* [2008]). The gross aspects of the observations are reproduced in the CTL run, which features a band of diurnal anomalies in meridional wind (Fig. 2) that maximize between 12 and 14 LT.

The latitudinal distribution of the migrating component of the diurnal cycle in surface pressure is quantitatively similar to the observed [*Haurwitz*, 1965], with a peak amplitude of around 0.6 hPa decreasing polewards and a maximum around 05 LT (Fig. 2), which in the model are surface-trapped up to an altitude of around 5 km (Fig. 3). The peak is between 5°N and 15°S approximately coincident with the declination subsolar latitudes of 5°S-15°S for this time of

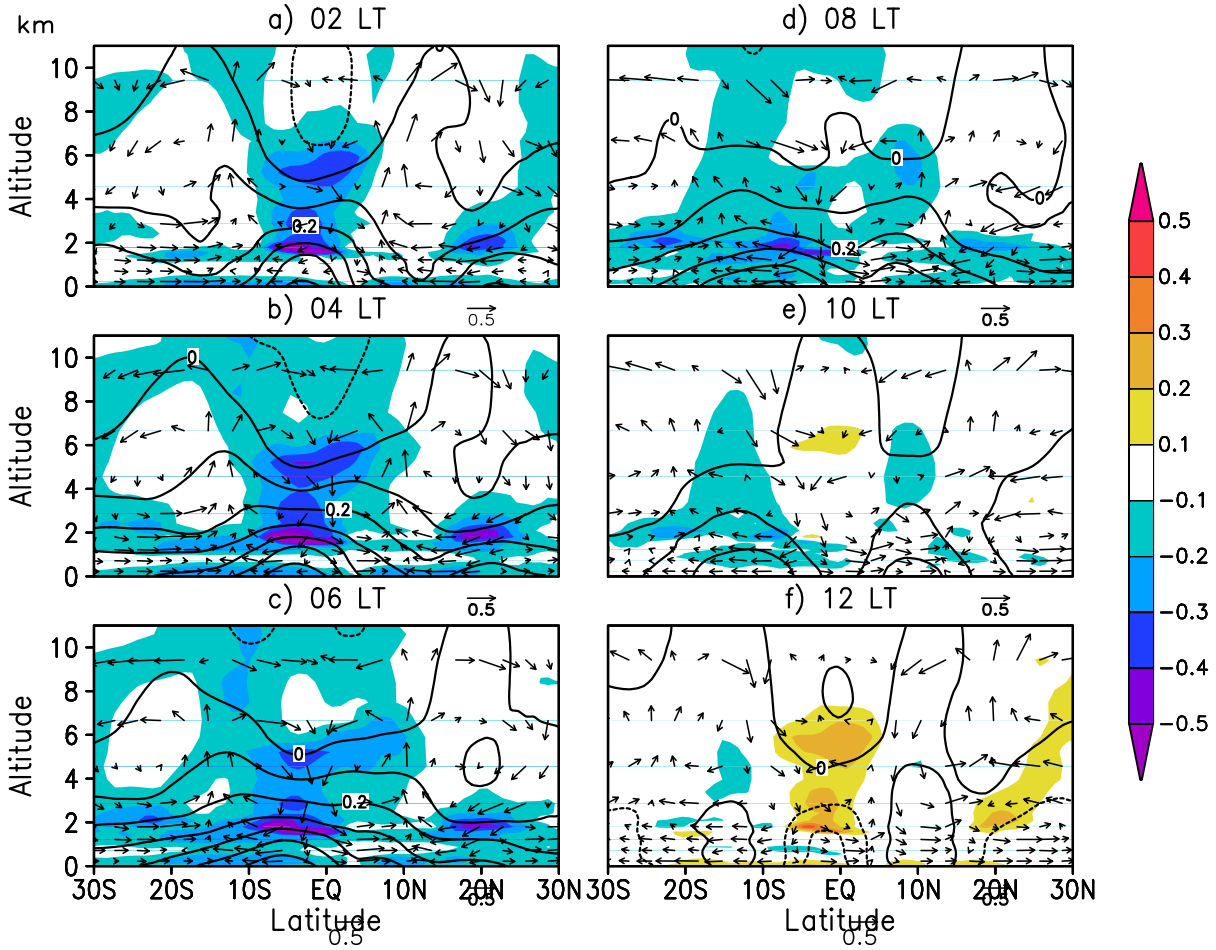

Figure 3. Latitude-altitude sections of diurnal components in temperature (shading, °C), pressure (contours, hPa) and meridional/vertical wind (scale in m/s and cm/s, respectively) from the CTL run, zonally averaged over the ocean between 150 and 110°W according to local time. Altitude is in km.

year. The model results also present polewards features with a latitudinal wavelength of around 20 degrees and amplitudes of up to 0.2 hPa (e.g. Fig. 3e), associated with more equatorially-confined amplitudes than in *Haurwitz* [1965], although the details are sensitive to the convective scheme.

The migrating component of the diurnal cycle of temperature has the largest amplitudes at altitudes between 2 and 7 km, where the lowest temperatures occur around 04 LT (Fig. 3), consistent with thermal driving of the meridional circulation. The Kain-Fritsch scheme produces a deeper diurnal cycle in temperature than Grell (not shown), probably due to the higher simulated upper tropospheric specific humidity (2-4 times greater in the mean within 20° from the equator between altitudes of 6 and 10 km), allowing for shortwave forcing at higher altitudes.

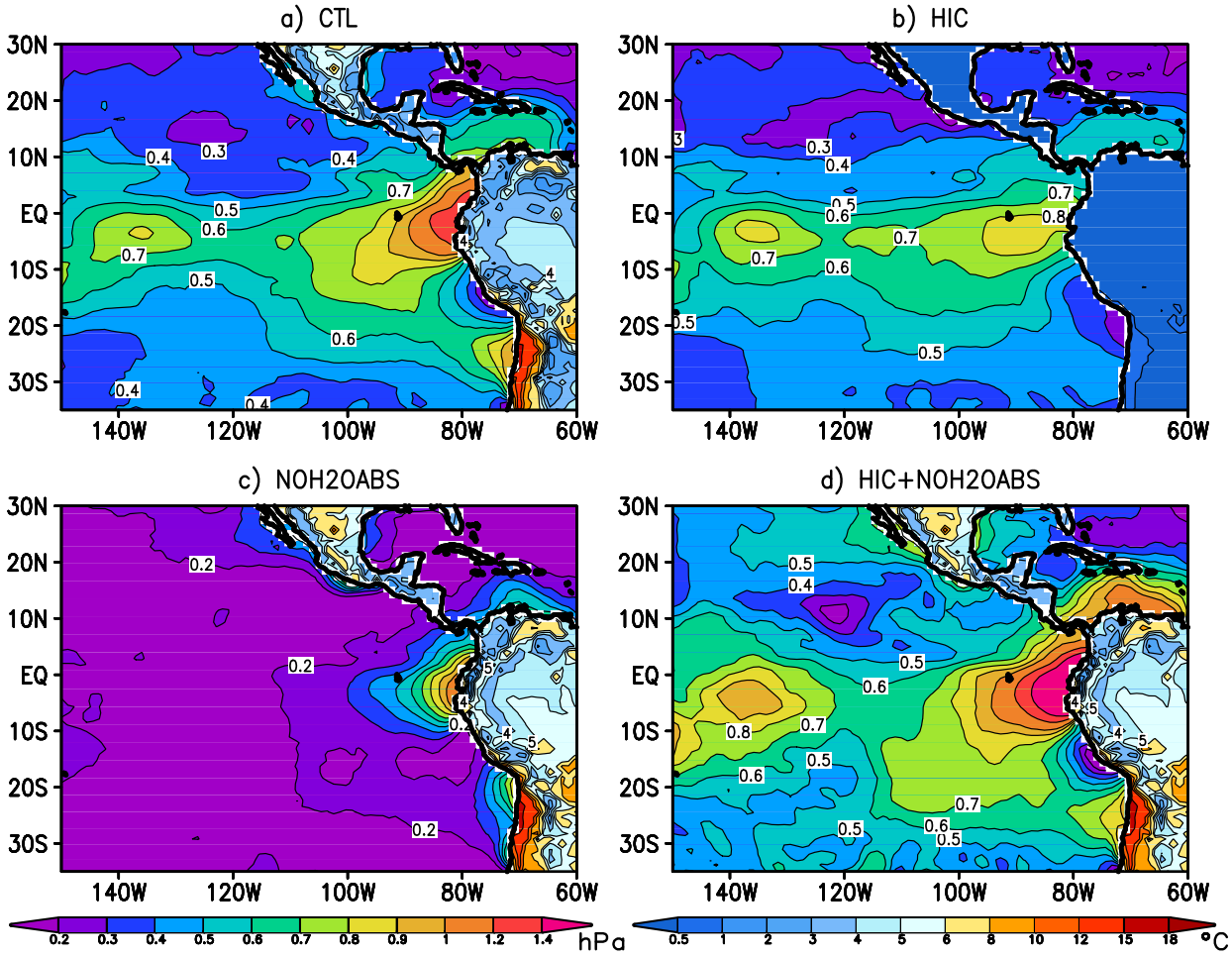

Figure 4. Amplitude of the simulated diurnal cycle in near-surface air pressure over the ocean (hPa) and in land surface temperature (°C) for the a) CTL, b) HIC, and c) NOH2OABS experiments, as well as d) the amplitudes of the sum of the diurnal components from the HIC and NOH2OABS experiments.

With the perturbed experiments we can discriminate the thermotidal effects from the extended sea-breeze forced by solar land-heating, as we note from the similarity of the diurnal amplitude in near-surface pressure in Figs. 4a and 4d, which indicates that the diurnal variability in CTL can be approximately expressed as the linear combination of HIC and NOH2OABS. As expected, the diurnal amplitude in HIC (Fig. 4b) depicts the thermotidal effect, with strongly reduced diurnal cycle in land surface temperature (cf. Figs. 4a and b) and approximately zonal distribution of amplitudes between 15°S and 5°N over the ocean. On the other hand, the NOH2OABS run (Fig. 4c) depicts the extended sea-breeze effect, with the highest amplitudes adjacent to the coast, explaining a large fraction of the amplitude seen in CTL in this region (cf. Fig. 4a). However, west of the coast of South America within 10°S-10°N, the amplitudes are largest and extend around 2000 km westward, but since the model overestimates the magnitude relative to observations (cf. Fig. 1a and b), we can only say that this effect and the thermotidal forcing are probably similar in importance. This overestimation is most likely associated with the land-heating effect, as the thermotidal response is expected to show relatively small variations in the zonal direction. On the other hand, south of 15°S and within 500 km from the coast, the land forcing is dominant and the diurnal cycle propagates poleward at around 28 m/s like a Kelvin wave

(i.e. in-phase northerly wind and high pressure anomalies, null zonal wind anomaly, and a zonal scale coincident with the Rossby radius based on the propagation speed; Fig. 2; see *Muñoz* [2008] for more details on this region). Within 500 km from the coast west of Central America, north of 10°N, the diurnal cycle behaves more like a traditional sea-breeze (Fig. 2), although further to the west the model does not adequately depict the variability (cf. Fig. 1a and b).

The CTL run also features a diurnal cycle in precipitation in the Intertropical and South Pacific convergence zones (ITCZ and SPCZ, respectively), peaking around 01 LT and with an amplitude on the order of 20-30% of the mean, although radar observations in the ITCZ show that it is closer to 05 LT and 6% [*Liu and Zipser*, 2008]. This diurnal cycle is also present in the HIC but not in the NOH2OABS run, indicating that the clear-sky shortwave forcing is essential, in contrast to mechanisms that rely on cloud effects [e.g. *Gray and Jacobson*, 1977; *Randall et al.*, 1991]. Since the models with the Grell and Kain-Fritsch cumulus schemes both simulate the thermotidal circulation but only Grell simulates a diurnal cycle in convection, it seems unlikely that the latter is directly driven by the former. A possible mechanism is the diurnal reduction of precipitation due to column stabilization by clear-sky shortwave heating of the mid-troposphere. This is similar to the *Randall et al.* [1991] mechanism, but with water vapor playing the key radiative role instead of clouds.

4. Conclusions and discussion

The numerical experiments indicate that the diurnal cycle of the open-ocean surface winds in the tropical Pacific and probably most of the tropics are forced by shortwave absorption by tropospheric water vapor as explained by thermotidal theory, whereas close to the coasts the extended sea-breeze driven by the diurnal solar heating of the land surface is of the same order. The importance of the forcing associated with the diurnal cycle in sea surface temperature [*Deser and Smith*, 1998] has not been directly tested, but there does not appear to be a need to invoke it.

The atmospheric shortwave forcing has a vertical distribution that depends on the humidity distribution, but clouds could also affect it. For instance, a maximum in clear sky heating at the mid-troposphere, could be shifted to the tropopause by the presence of thick high clouds [*Lieberman et al.*, 2003].

Under greenhouse global warming, the mean tropospheric shortwave absorption increases due to increased water vapor [*Takahashi*, 2009], so the diurnal cycle in surface winds and precipitation could be expected to increase as well.

The blocking effect of the Andes modifies the extended sea-breeze so that south of 15°S it results in poleward-propagating Kelvin waves, whereas off central Peru the cycle is weakened. The topographically-modified extended sea-breeze and the thermal tide all contribute to the diurnal cycle of winds in the southeast Pacific and understanding the cycle in any particular location within it will require further in-depth studies.

Despite the limitations, the model simulations suggest a local forcing mechanism for the diurnal cycle of precipitation in the ITCZ and SPCZ. Diurnal reduction of convection would result from shortwave absorption by water vapor heating the mid-troposphere and stabilizing the column. In models, however, the effectiveness of this mechanism is sensitive to the convective parameterization scheme.

Acknowledgments. Figures and calculations were made with the GNU Octave and GrADS software. Quikscat gridded data was provided by Remote Sensing Systems. NCEP/NCAR Reanalysis and NOAA OI SST data were provided by NOAA ESRL. The author thanks Dr. Clara Deser and an anonymous reviewer for their constructive comments.

References

Arritt, R. W. (1989), Numerical modelling of the offshore extent of sea breezes, *Q. J. R. Met. Soc. 115*, 547–570.

Blackadar, A. K. (1976), High resolution models of the planetary boundary layer. *Advances in Environmental Sciences and Engineering*, *1*, 50-58.

Dai A., and Deser C. (1999), Diurnal and semidiurnal variations in global surface wind and divergence fields. *J. Geophys. Res. 104*, 31109–31125.

Deser C., and Smith, C. A. (1999), Diurnal and semidiurnal variations of the surface wind field over the tropical Pacific Ocean *J. Climate 11*, 1730–1748.

Garreaud, R. D., and Muñoz, R. (2004), The diurnal cycle in circulation and cloudiness over the subtropical southeast Pacific: A modeling study, *J. Climate 17*, 8, 1699–1710.

Gayno, G. A. (1994), Development of a higher-order, fog-producing boundary layer model suitable for use in numerical weather prediction, M.S. thesis, Department of Meteorology, The Pennsylvania State University, 104 pp.

Gille, S., Llewellyn, S. G., and Lee, S. M. (2003), Measuring the sea breeze from QuikSCAT scatterometry, *Geophys. Res. Lett. 30*, 3, 1114, doi:10.1029/2002GL016230.

Gray, W. M., and Jacobson, R. W. (1977), Diurnal variation of deep cumulus convection, *Mon. Wea. Rev. 105*, 1171–1188.

Grell, G. A. (1993), Prognostic evaluation of assumptions used by cumulus parameterizations, *Mon. Wea. Rev. 119*, 5–31.

Grell, G. A., Dudhia, J., and Stauffer, D. R. (1995), A description of the fifth-generation Penn State/NCAR mesoscale model (MM5). *NCAR Technical Note 398*.

Hack, J. J., B. A. Boville, B. P. Briegleb, J. T. Kiehl, P. J. Rasch, and D. L. Williamson (1993), Description of the NCAR Community Climate Model (CCM2). *NCAR Technical Note* NCAR/TN-382+STR, 120 pp.

Haurwitz, B. (1965), The diurnal surface-pressure oscillation, *Arch. Met. Geoph. Biokl. A* 14, 363-379.

Kain, J. S., and J. M. Fritsch (1993), Convective parameterization for mesoscale models: The Kain-Fritsch scheme. *The representation of cumulus convection in numerical models*, K. A. Emanuel and D. J. Raymond, Eds., Amer. Meteor. Soc., 246 pp.

Lieberman, R. S., D. A. Ortland, and E. S. Yarosh (2003), Climatology and interannual variability of diurnal water vapor heating, *J. Geophys. Res.*, *108*, D3, 4123, doi:10.1029/2002JD002308.

Lindzen, R. S. (1967), Thermally driven diurnal tide in the atmosphere, *Q. J. R. Meteorol. Soc. 93*, 395, 18–42, doi:10.1002/qj.49709339503.

Liu, C. and E. J. Zipser (2008), Diurnal cycles of precipitation, clouds, and lightning in the tropics from 9 years of TRMM observations. *Geophys. Res. Lett.* 35, L04819, doi:10.1029/2007GL032437.

Muñoz, R. C. (2008), Diurnal cycle of surface winds over the subtropical southeast Pacific, *J. Geophys. Res.*, *113*, D13107, doi:10.1029/2008JD009957.

Rahn, D. A., and Garreaud, R. (2010), Marine boundary layer over the subtropical southeast Pacific during VOCALS-REx – Part 1: Mean structure and diurnal cycle, *Atmos. Chem. Phys 10*, 4491–4506, doi:10.5194/acp-10-4491-2010.

Randall, D. A., Harshvardhan, Dazlich, D. A. (1991), Diurnal variability of the hydrological cycle in a general circulation model, *J. Atmos. Sci. 48*, 1, 40–62.

Rotunno, R. (1983), On the linear theory of the land and sea breeze, *J. Atmos. Sci. 40*, 8, 1999–2009.

Simpson, J. E. (1994), *Sea Breeze and Local Wind*, Cambridge University Press, 234 p.

Takahashi, K. (2009) The global hydrological cycle and atmospheric shortwave absorption in climate models under CO_2 forcing. *J. Climate 22*, 21, 5567–5675.

Ueyama, R., and Deser C. (2008), A climatology of diurnal and semidiurnal surface wind variations over the tropical Pacific Ocean based on the tropical atmosphere ocean moored buoy array *J. Climate 21*, 4, 593–607.

Wood, R., Köhler, M., Bennartz, R., O'Dell, C. (2009), The diurnal cycle of surface divergence over the global oceans *Q. J. R. Met. Soc. 135*, 1484–1493, doi:10.1002/qj.451.

Ya, H., and Anthes, R. (1987), The effect of latitude on the sea breeze, *Mon. Wea. Rev. 115*, 936–956.

K. Takahashi, Instituto Geofísico del Perú, Perú (ken.takahashi@igp.gob.pe)